Electronic Supplementary Material (ESI) for New Journal of Chemistry.

Electronic Supplementary Information

Representation of a photosensitive Schottky barrier diode made with hetero-dinuclear cobalt(III)/sodium building block

Sourav Roy[a], Soumi Halder[b], Arka Dey[b,c], Klaus Harms[d], Partha Pratim Ray[b]* and Shouvik Chattopadhyay[a]*

[a]Department of Chemistry, Inorganic Section, Jadavpur University, Kolkata - 700032, India. Tel: +9133-2457-2941; E-mail: shouvik.chem@gmail.com

[b]Department of Physics, Jadavpur University, Kolkata-700012, India. E-mail: partha@phys.jdvu.ac.in; Fax: +91 3324138917

[c]Department of Condensed Matter Physics and Material Sciences, S. N. Bose National Centre for Basic Sciences, Block JD, Sec. III, Salt Lake, Kolkata 700106, India.

[d]Fachbereich Chemie, Philipps-Universität Marburg, Hans-Meerwein-Strasse, D-35032 Marburg, Germany

---

Table S1: Selected bond lengths (Å) of the complex.

Co(1)-O(1)	1.907(9)	Na(1)-O(1)	2.312(10)
Co(1)-O(2)	1.897(9)	Na(1)-O(2)	2.311(10)
Co(1)-N(1)	1.925(11)	Na(1)-O(3)	2.487(11)
Co(1)-N(2)	1.918(10)	Na(1)-O(4)	2.446(10)
Co(1)-N(3)	1.980(11)	Na(1)-O(5)	2.233(11)
Co(1)-N(6)	1.961(11)		

Table S2: Selected bond angles (°) of the complex.

O(1)-Co(1)-O(2)	83.15(4)	N(2)-Co(1)-N(6)	89.49(4)
O(1)-Co(1)-N(1)	91.49(4)	N(3)-Co(1)-N(6)	177.79(5)

O(1)-Co(1)-N(2)	173.69(4)	O(1)-Na(1)-O(2)	66.18(3)
O(1)-Co(1)-N(3)	91.06(4)	O(1)-Na(1)-O(3)	65.70(3)
O(1)-Co(1)-N(6)	90.82(4)	O(1)-Na(1)-O(4)	128.01(4)
O(1)-Co(1)-N(1)	174.64(4)	O(1)-Na(1)-O(5)	140.59(4)
O(2)-Co(1)-N(2)	90.54(4)	O(2)-Na(1)-O(3)	126.89(4)
O(2)-Co(1)-N(3)	89.48(4)	O(2)-Na(1)-O(4)	65.99(3)
O(2)-Co(1)-N(6)	91.90(4)	O(2)-Na(1)-O(5)	146.38(4)
N(1)-Co(1)-N(2)	94.82(5)	O(3)-Na(1)-O(4)	137.44(4)
N(1)-Co(1)-N(3)	90.55(5)	O(3)-Na(1)-O(5)	86.67(4)
N(1)-Co(1)-N(6)	88.23(4)	O(4)-Na(1)-O(5)	91.38(4)
N(2)-Co(1)-N(3)	88.77(4)		

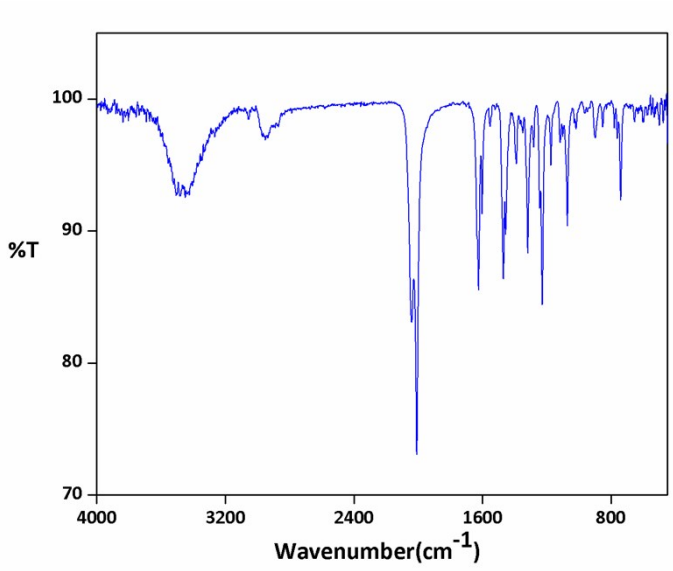

Fig S1: IR spectrum of the complex.

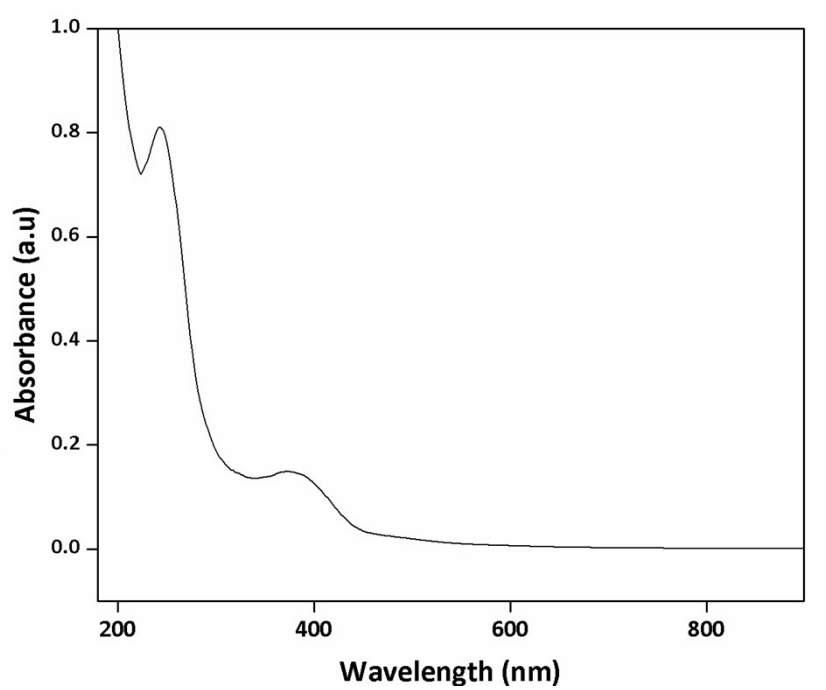

Fig S2: UV-Vis spectrum of the complex.

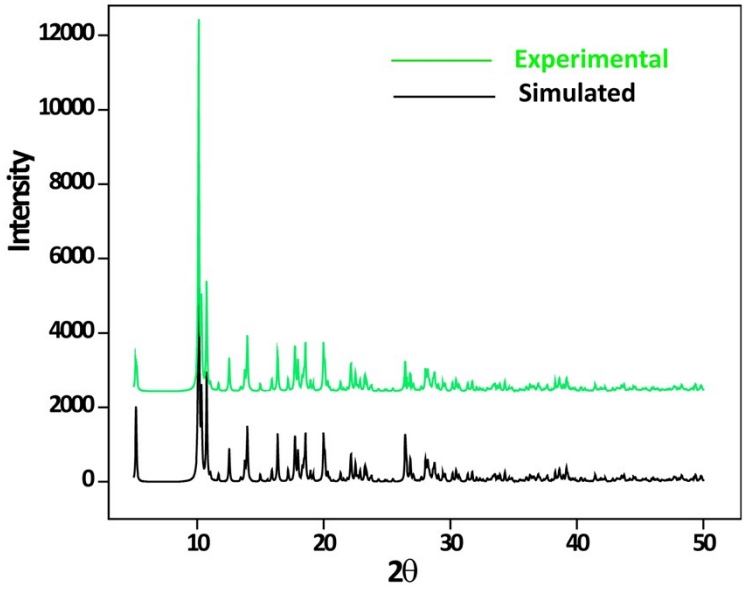

Fig. S3: Experimental and simulated PXRD patterns of the complex confirming purity of the bulk material.

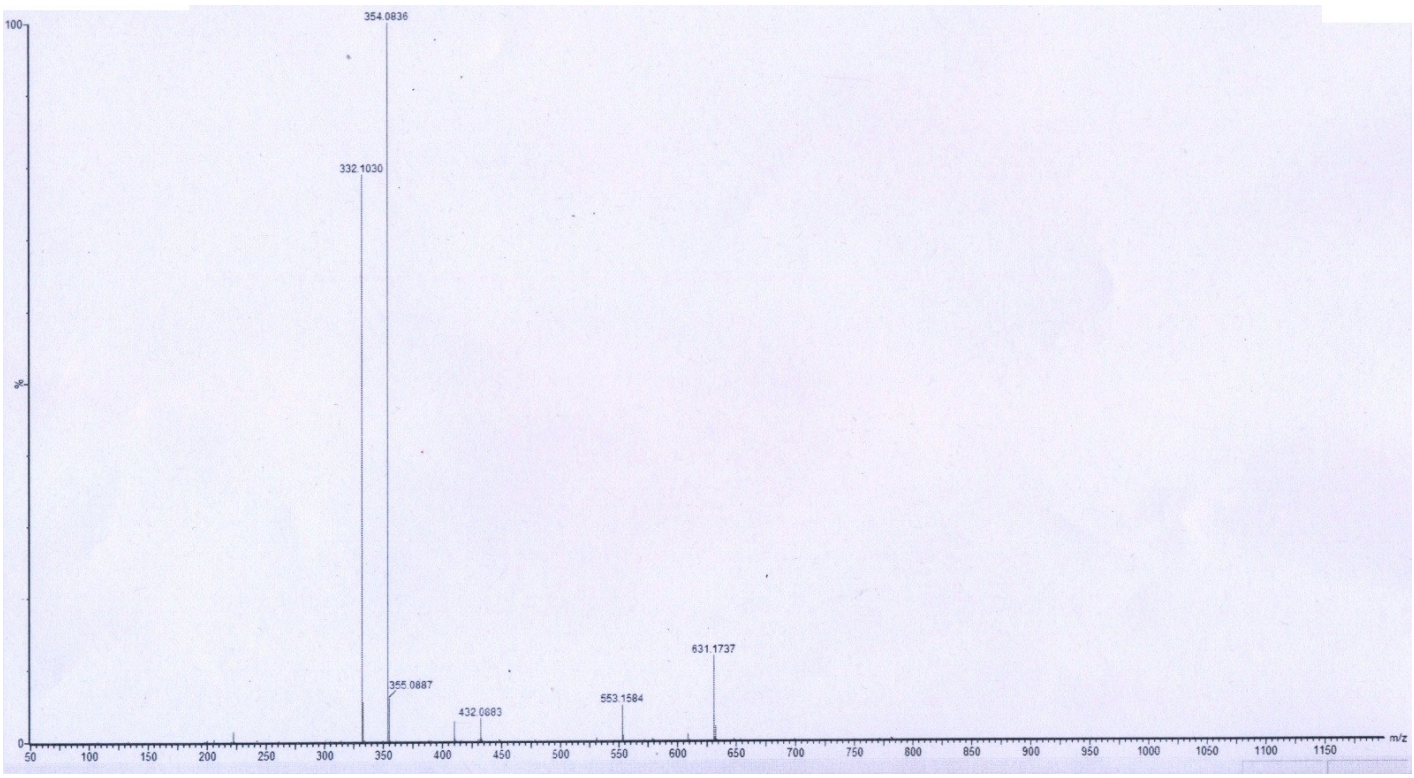

Fig. S4: Mass spectrum of the complex.

Calculation based on Bond Valence Sum method

Bond Valence Sum (BVS) method has been used to determine the oxidation state of metal ions in solids based on crystallographically determined metal-ligand bond distance.[1,2] Bond valences (s_{ij}) are calculated according to equation S1.

$$s_{ij} = \exp[(r_0 - r_{ij})/b] \text{.....(S1)}$$

Where, *i* = donor centre; *j* = metal centre; r_0 = reported bond length between *i* and *j*; r_{ij} = the observed bond length, s_{ij} = the valence of a bond between two atoms *i* and *j*. and b is usually taken to be 0.37.

Bond Valence Sum is calculated according to the equation S2, The valence sum rule (Pauling's second rule) is defined

$$z_j = \sum_i s_{ij} \quad \text{.....(S2)}$$

Where, z_j is the valence of atom *j* connecting *i–j* bonds with all neighbouring *i* atoms.

The bond valence sum (BVS) calculation is performed to calculate the oxidation state of cobalt in the complex. The result is little higher[3,4] for the oxidation state of cobalt(III) which indicates either possible steric constraints, excessive thermal motion, problems with the crystal structure report, or some combination of all of these effects. All the parameters and calculated values related to BVS calculation are gathered in Table **S3**.

Table S3: Bond valence sum calculation and the related parameters for the complex.

i–j **reported**	r_0	***i–j*** **this complex**	r_{ij}	s_{ij}	z_j
O–Co^{3+}	1.692	O(1)–Co(1)	1.907(9)	0.5593	
O–Co^{3+}	1.692	O(2)–Co(1)	1.897(9)	0.5746	
N–Co^{3+}	1.840	N(1)–Co(1)	1.925(11)	0.7947	
N–Co^{3+}	1.840	N(2)–Co(1)	1.918(10)	0.8099	4.14
N–Co^{3+}	1.840	N(3)–Co(1)	1.980(11)	0.6850	
N–Co^{3+}	1.840	N(6)–Co(1)	1.961(11)	0.7210	

Where *i* = donor centre; *j* = metal centre; r_0 = reported bond length between *i* and *j*; r_{ij} = the observed bond length; s_{ij} = the valence of a bond between two atoms *i* and *j* and z_j = the valence of atom *j* connecting *i–j* bonds with all neighbouring *i* atoms.

Hirshfeld surfaces

Hirshfeld surfaces of the complex, mapped over d_{norm}, shape index and curvedness, have been shown in Fig. S5. Red spots on the d_{norm} surface (Fig. S5) indicate the interaction between nitrogen and hydrogen atoms. O···H and N···H contacts have also observed in the Hirshfeld surfaces as smaller visible spots of light colour. The intermolecular interactions appearing as distinct spikes in the 2D fingerprint plot have been shown in Fig. S5. Interesting N···C and N···H contacts have been observed which further assist the formation of supramolecular C-H···π(N_3) interactions in the solid state of the complex.

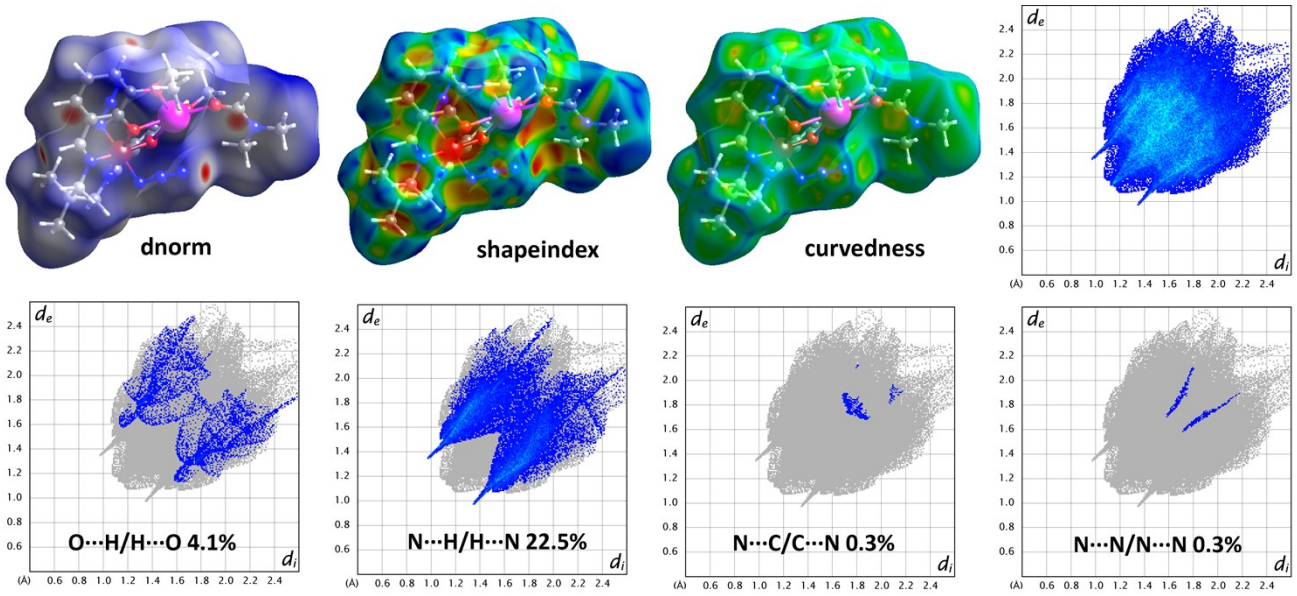

Fig. S5: Hirshfeld surfaces (above) and fingerprint plots (below): Broken down into contributions from specific pair of atom types for the complex.

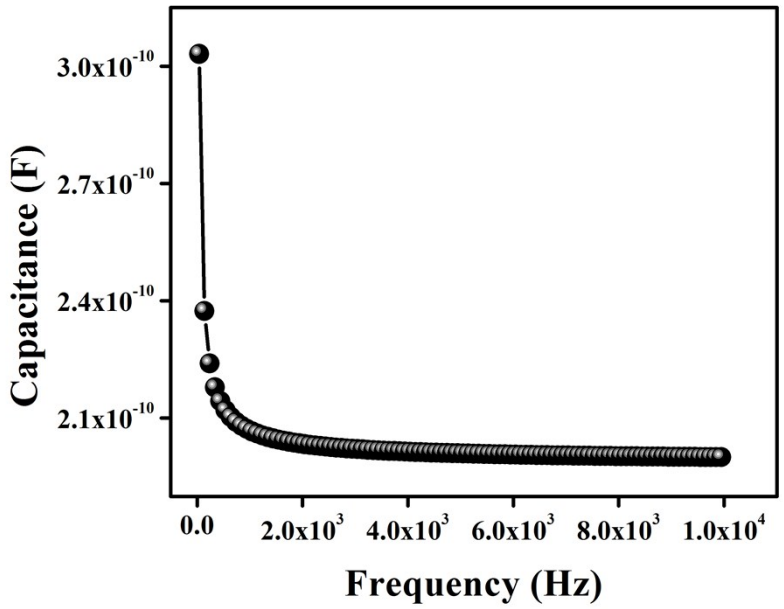

Fig. S6: Capacitance *vs.* frequency graph for determination of dielectric constant.

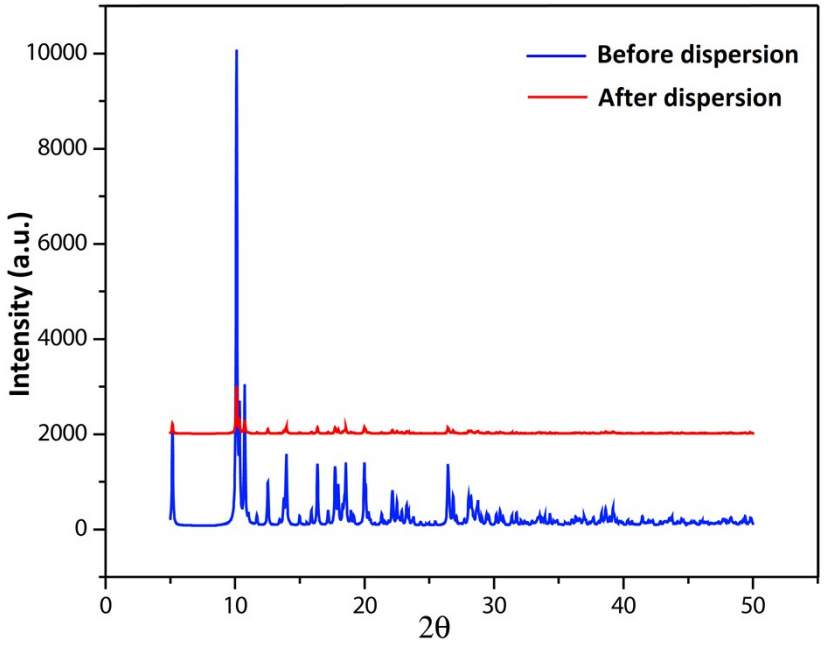

Fig. S7: PXRD patterns of the complex before and after dispersion in DMF.

Cyclic Voltammetry

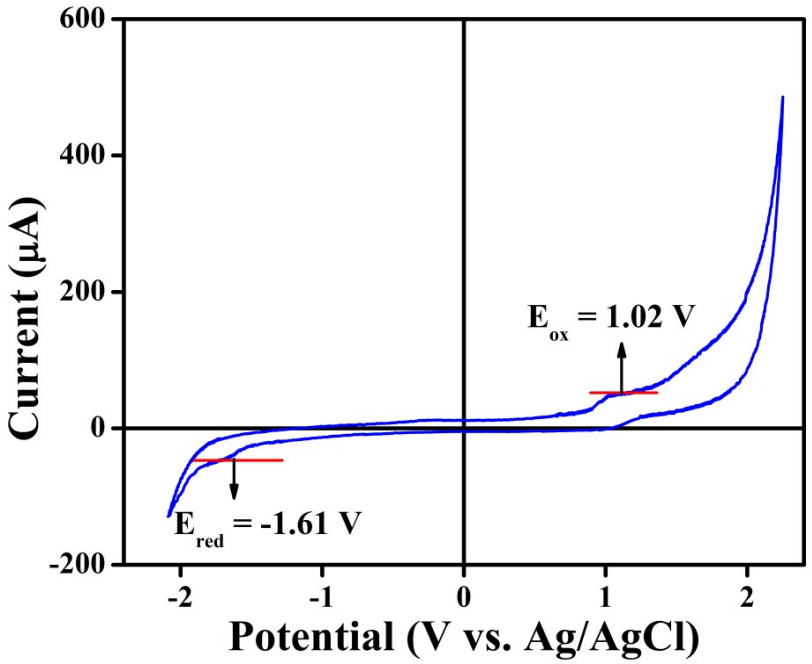

Fig S8: Cyclic Voltammetry spectrum of the complex.

Electrochemical study has been performed for better approximation of the band position by investigating the oxidation and reduction peaks of the complex. The electrochemical measurements were carried out using a Gamry reference 750 potentiostat in a three-electrode configuration. The working electrode was a photocatalyst powder-modified glassy carbon electrode (GCE) (3 mm diameter), the reference electrode was an Ag/AgCl (in 3 M NaCl) electrode, and the counter electrode was a platinum wire. The cyclic voltammetry curve of the complex in DMF has been shown in Fig. S8. The above spectrum depicts the oxidation and reduction potential of complex as 1.02 V and -1.61 V respectively.

AFM analysis

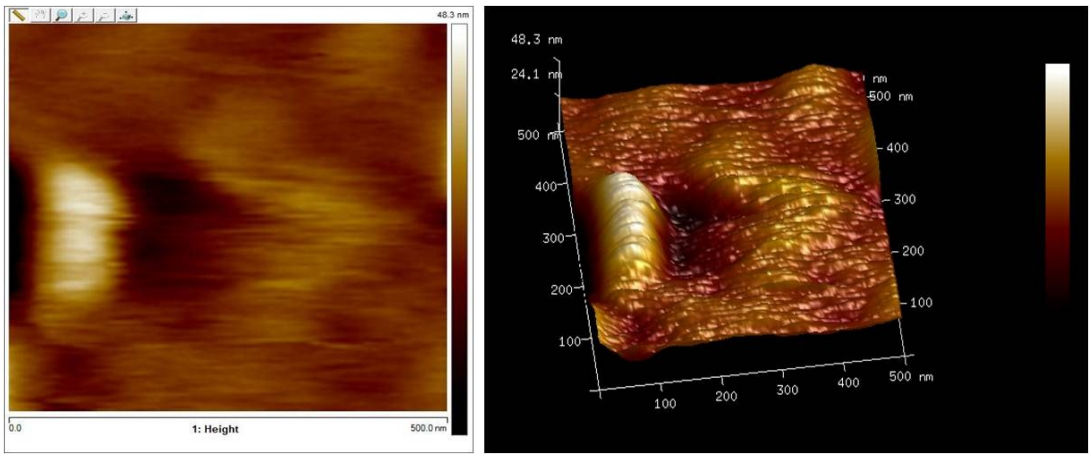

Fig S9: Atomic force micrograph of the top of the thin film of the complex.

The AFM micrograph of the complex after spin coating of it on ITO substrate has been presented in Fig S9. From this micrograph the RMS value of the surface roughness has been obtained as 5.16 nm.

Table S4: Previously reported X-ray characterized photosensitive complexes.

Complex	**Conductivity in dark (S m^{-1})**	**Conductivity under light (S m^{-1})**	**Photosensitivity**	**Ref**
$[CdL^1(\mu\text{-}_{1,3}\text{-}SCN)_2]_n$	1.01×10^{-8}	2.16×10^{-8}	14.36	5
$[Cu_2(adc)(4\text{-}pic)_6(H_2O)_4][ClO_4]_2$	8.21×10^{-4}	11.84×10^{-4}	1.83	6
$\{[Zn(adc)(4\text{-}spy)_2(H_2O)_2]\}_n$	5.12×10^{-4}	16.48×10^{-4}	1.96-2	7
$\{[Cd(adc)(4\text{-}spy)_2\text{-}(H_2O)_2]\}_n$	6.54×10^{-4}	28.77×10^{-4}	3.5	7

[Cd(2,2'-dsb)(4-nvp)(DMF)(H_2O)]	6.60×10^{-4}	10.71×10^{-4}	0.54	8
$[Cu_2(L^1)_2(\mu\text{-}_{1,3}\text{-}SCN)_2]_n$	3.63×10^{-5}	4.13×10^{-5}	2.83	9
$[\{CuL^2Na\}_2(\mu\text{-}_{1,1,3}\text{-}NCS)HgCl_2(\mu\text{-}_{1,3}\text{-}NCS)]_n$	1.48×10^{-6}	8.40×10^{-5}	57	10
$[(NCS)Pb(H_2O)L^2Ni(NCS)]_n$	6.02×10^{-6}	3.47×10^{-5}	5.76	11
$[(NCS)(H_2O)NiL^3Pb(DMF)Cl]$	7.47×10^{-4}	23.12×10^{-4}	4.86 ~ 5	12
$[Cd_4(L^4)_2(NCO)_6]_n$	8.26×10^{-2}	22.07×10^{-2}	2.56	13
$[Zn(adc)(4\text{-}nvp)_2(H_2O)_2]_n$	9.29×10^{-4}	16.58×10^{-4}	2.73–3	14
$[(N_3)CoL(\mu\text{-}_{1,3}\text{-}N_3)Na(DMF)]$	8.24×10^{-5}	14.03×10^{-5}	2.31	This work

Where, HL^1 = 2-(2-(ethylamino)ethyliminomethyl)-6-ethoxyphenol; H2adc = acetylenedicarboxylic acid; 4-pic = 4-picolene; 4-spy = 4-styrylpyridine; $H_2$2,2'-dsb = 2,2'-disulfanediyldibenzoic acid (2,2'-dsba) and 4-nvp = 4-(1-naphthylvinyl)pyridine; H_2L^2 = [N,N'-bis(3-methoxysalicylidene)propane-1,3-diamine]; H_2L^3 = [N,N'-bis(5-bromo-3-methoxysalicylidene)-2,2-dimethylpropane-1,3-diamine]; HL^4 = [2-methoxy-6-((quinolin-8-ylimino)methyl)phenol]; H_2adc = acetylenedicarboxylic acid, 4-nvp = 4-(1-naphthylvinyl)pyridine]; H_2adc = acetylenedicarboxylic acid, 4-pic = 4-picolene.

References

[1] I. D. Brown and D. Altermatt, *Acta Crystallogr*., 1985, **B41**, 244-247.

[2] H. H. Thorp, *Inorg. Chem*., 1992, **31**, 1585-1588.

[3] A. Banerjee and S. Chattopadhyay, *Polyhedron*, 2019, **159**, 1–11.

[4] S. Majumder, S. Mondal, P. Lemoine and S. Mohanta, Dalton *Trans.*, 2013, **42**, 4561-4569.

[5] S. Roy, A. Dey, P. P. Ray, J. Ortega-Castro, A. Frontera and S. Chattopadhyay, *Chem. Commun.,* 2015, **51**, 12974-12976.

[6] B. Dutta, A. Dey, K. Naskar, F. Ahmed, R. Purkait, S. Islam, S. Ghosh, C. Sinha, P. P. Ray and M. H. Mir, *New J. Chem*., 2018, **42**, 8629−8637.

[7] B. Dutta, A. Dey, K. Naskar, S. Maity, F. Ahmed, S. Islam, C. Sinha, P. Ghosh, P. P. Ray and M. H. Mir, *New J. Chem*., 2018, **42**, 10309−10316.

[8] B. Dutta, R. Jana, C. Sinha, P. P. Ray and M. H. Mir, *Inorg. Chem. Front*., 2018, **5**, 1998−2005.

[9] S. Khan, S. Halder, P. P. Ray, S. Herrero, R. Gonzalez-Prieto, M. G. B. Drew and S. Chattopadhyay, *Cryst. Growth Des.,* 2018, **18 (2)***,* 651-659.

[10] S. Roy, S. Halder, M. G. B. Drew, P. P. Ray and S. Chattopadhyay, *New J. Chem.,* 2018, **42**, 15295-15305.

[11] S. Roy, S. Halder, M. G. B. Drew, P. P. Ray and S. Chattopadhyay, *ACS Omega,* 2018, **3**, 12788−12796.

[12] S. Roy, A. Dey, M. G. B. Drew, P. P. Ray and S. Chattopadhyay, *New J. Chem.,* 2019, **43**, 5020-5031.

[13] P. Ghorai, A. Dey, P. Brandaõ, J. Ortega- Castro, A. Bauza, A. Frontera, P. P. Ray and A. Saha, *Dalton Trans*., 2017, **46**, 13531–13543.

[14] B. Dutta, A. Dey, S. Maity, C. Sinha, P. P. Ray and M. H. Mir, *ACS Omega,* 2018, **3**, 12060−12067.